Editors' Suggestion

Anapole Meta-Atoms: Nonradiating Electric and Magnetic Sources

Esmaeel Zanganeh,[1] Andrey Evlyukhin,[2,3,*] Andrey Miroshnichenko,[4,†] Mingzhao Song,[5,1] Elizaveta Nenasheva,[6] and Polina Kapitanova[1,‡]

[1]School of Physics and Engineering, ITMO University, Saint Petersburg 197101, Russia
[2]Institute of Quantum Optics, Leibniz University Hannover, Welfengarten 1, 30167 Hannover, Germany
[3]Moscow Institute of Physics and Technology, Dolgoprudny 141700, Russia
[4]School of Engineering and Information Technology, University of New South Wales Canberra, Australian Capital Territory 2600, Australia
[5]College of Information and Communication Engineering, Harbin Engineering University, Harbin 150001, China
[6]Ceramics Company Limited, 10, Kurchatova Street, Saint Petersburg 194223, Russia

(Received 24 February 2021; accepted 20 July 2021; published 27 August 2021)

The existence of classical nonradiating electromagnetic sources is one of the puzzling questions to date. Here, we investigate radiation properties of physical systems composed of a single ultrahigh permittivity dielectric hollow disk excited by electric or magnetic pointlike dipole antennas, placed inside the inner bore. Using analytical and numerical methods, we demonstrate that such systems can support anapole states with total suppression of far-field radiation and thereby exhibit the properties of electric or magnetic nonradiating sources. It is shown that the suppression of the far-field radiated power is a result of the destructive interference between radiative contributions of the pointlike dipole antennas and the corresponding induced dipole moments of the hollow disk. The experimental investigation of the nonradiating electric source has been performed to confirm our theoretical predictions. Our results pave the way to create and realize compact nonradiative sources for applications in modern wireless power transfer systems, sensors, RFID tags, and medical technologies.

DOI: 10.1103/PhysRevLett.127.096804

One of the common understandings is that, according to Maxwell's equations, any confined configuration of alternating currents should emit electromagnetic radiation to the far field. It was a stumbling block explaining matter's stability, consisting of atoms and molecules. This fact led Bohr to the formulation of his famous postulates, which laid the foundation of quantum mechanics. But, the question remained open, and numerous efforts were undertaken to find the classical (macroscopic) analog of nonradiating confined current configurations. If they exist, such states can be considered as *meta-atoms*, in analogy with realistic atoms, governed by quantum mechanics. They should be able to trap and confine the electromagnetic (EM) energy in finite volumes indefinitely without far-field emission. One of the examples is a radially oscillating charged spherical shell, which is not realizable. Other approach to meta-atom realizations with "unusual" EM properties [1] can be based on the concept of the toroidal dipole response [2] and anapole states [3,4] which generate no far-field radiation [5].

In electrodynamic problems, anapole states are defined as destructive interference between waves generated by Cartesian and toroidal multipoles [2,5] presented in the long-wavelength approximation (LWA) [6,7]. In this context, toroidal multipoles represent subsets of the exact electric and magnetic multipoles [8]. For example, the toroidal dipole appears as a third-order multipole in the Taylor expansion of the electromagnetic potentials and is a part of exact electric dipole moments defined in the Cartesian or spherical harmonics presentations [9,10]. The realization of an anapole state in a system leads to the formation of nonscattering and nonradiating (NR) sources [4,5,11]. The general theory about NR sources was formulated by Devaney and Wolf in 1973 [12].

In scattering and radiation or emission problems, enormous efforts have been done to realize and experimentally verify the NR-type sources [3,5,11,13–25]. Recently, an NR source composed of four high refractive index dielectric cylinders excited by an electric dipole antenna has been reported [24]. It was demonstrated that a strong induced electric toroidal dipole (ETD) inside the cylinders leads to radiation suppression through destructive interference with electric dipole (ED) radiation from the dipole antenna creating an anapole state, as schematically illustrated in Fig. 1(a). Another paper theoretically studied a NR source that arises from ED cancellation between an electric pointlike antenna placed in near proximity to a subwavelength sphere and induced ED mode inside the sphere [25].

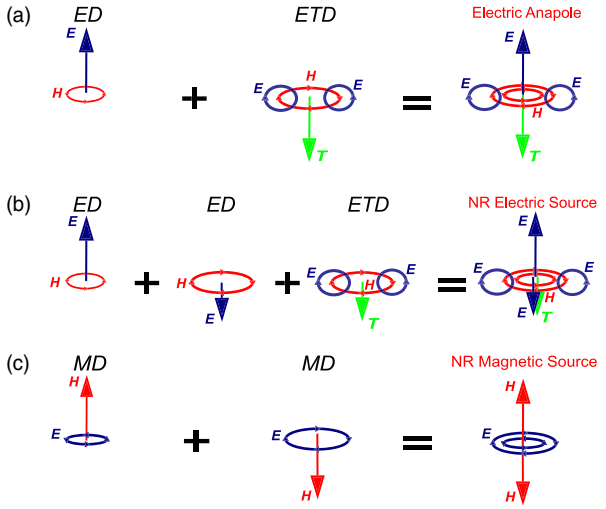

FIG. 1. The conceptual approaches to realize (a) electric anapole, (b) NR electric source, and (c) NR magnetic source.

In this Letter, we investigate meta-atoms supporting anapole states and exhibiting the properties of electric or magnetic NR sources as demonstrated in Figs. 1(b) and 1(c). We study two practical realization of NR sources as physical systems based on a single ultrahigh permittivity dielectric hollow disk excited by electric or magnetic pointlike dipoles placed inside the hollow disk. Our theoretical results of the simulated radiated power and near fields are obtained in CST MICROWAVE STUDIO2020. The Cartesian multipole expansion analysis in the LWA is performed to show the origin of NR sources explicitly. This approach is applied because the size of the system under study is much smaller that the wavelength of radiation. Here, we use a secondary multipole expansion approach [26] taking explicitly into account the contributions of various parts of the system. It also allows us to confirm that our results are consistent with Devaney-Wolf theorem on NR sources (see Sec. IV in Supplemental Material [27]). To prove out theoretical predictions, the experimental study of the NR electric source is provided.

First, we study the meta-atom based on an ultrahigh permittivity dielectric hollow disk with an electric dipole antenna inside, as depicted in Fig. 2(a). The meta-atom is much smaller than the wavelength of radiated waves; thus, only electric dipole contributions will determine the nonradiating regime. Being excited, the dipole antenna radiates EM waves as an ED mode and, correspondingly, induces a displacement current inside the dielectric hollow disk. By a proper design, the induced current radiates secondary EM waves as another ED and ETD which can interfere with the ED radiation of the dipole antenna destructively. It provides suppression of the total radiation and corresponds to realization of the NR electric source, as depicted in Fig. 1(b). The novelty lies in the fact that the ED moment of the dipole antenna also takes part in the creation of the anapole state.

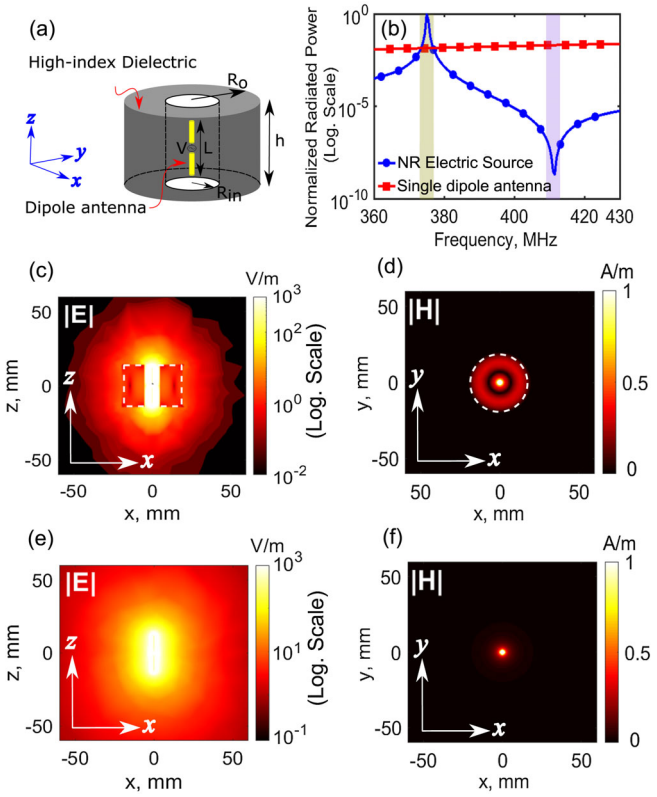

FIG. 2. (a) Schematic view of the NR electric source consisting of a dielectric hollow disk ($\varepsilon = 1000$, $\tan\delta = 2.5 \times 10^{-4}$, $R_0 = 20$ mm, $R_{in} = 5$ mm, and $h = 28$ mm) and short copper electric dipole antenna ($L = 25$ mm, wire diameter $= 1$ mm) placed in the hollow disk center. A discrete port with 50 Ω impedance is inserted into the 1 mm slit made in the dipole antenna center. (b) Simulated radiated power of the single dipole antenna in free space and NR electric source over the frequency. The results are normalized to the maximum radiated power of the NR electric source. (c),(d) Simulated electric and magnetic field distributions of the NR electric source. Here, the dashed white lines represent the border of the dielectric hollow disk. (e),(f) Simulated electric and magnetic field distributions of the single short copper electric dipole ($L = 25$ mm, 1 mm slit in the middle to allocate a 50 Ω port) in free space.

The radiated power and near-field distributions of the NR electric source were studied numerically and compared to the simulated characteristics of a single electric dipole antenna in free space (Fig. 2). The radiated power of the NR electric source has a maximum at the frequency of 375 MHz, that is, the resonance frequency of the dielectric hollow disk [see Fig. 2(b)]. We consider this state as radiative and provide its detailed discussion in Sec. I in Supplemental Material [27]. The almost zero radiated power is obtained at the frequency of 411 MHz. At this frequency, the radiated power is 7 orders of magnitude lower than the radiated power of the single dipole antenna in free space. It reveals a strong suppression of the far-field radiation and can serve as an indicator of the anapole state formation. One can see a strong confinement of the electric

field inside and around the NR electric source [see Fig. 2(c)] in contrast to the electric field of the single dipole antenna [Fig. 2(e)]. The magnetic field of the NR electric source is concentrated inside the volume of the dielectric disk and its entire bore [see Fig. 2(d)]. It indicates a strong redistribution compared to the fields of the single dipole antenna depicted in Figs. 2(e) and 2(f).

To gain a deeper understanding, we performed the Cartesian multipole expansion of the EM fields generated by the NR electric source [7,34,35] (see Supplemental Material Sec. III [27] for more information), and the results are shown in Figs. 3(a) and 3(b). The radiated power of the total electric dipole (ED + ETD) agrees well with the total radiated power [Fig. 3(a)]. Therefore, the contributions of only ED and ETD are enough to describe the radiated power. In this case, for the total radiated power P, one can write

$$P \sim |\mathbf{p}_0 + \mathbf{p}_1 - ik\mathbf{T}|^2 = |\mathbf{p}_0 + \mathbf{p}_1|^2 + k^2|\mathbf{T}|^2 + 2k\mathrm{Im}[\mathbf{T}(\mathbf{p}_0^* + \mathbf{p}_1^*)], \quad (1)$$

where $\mathbf{p}_0$ and $\mathbf{p}_1$ are the ED moments of the dipole antenna and the hollow disk, respectively, $\mathbf{T}$ is the ETD of the hollow disk, k is the wave number, and $*$ indicates the complex conjugation. It is important to emphasize that, for anapole state realization, it is necessary to include dipole moments of the dipole antenna in the total multipole decomposition. As a consequence, the total radiated power in Eq. (1) is determined by not only the direct contributions of the all dipole moments, but also their interference terms. Let us focus on the frequency 397 MHz, where the ED has minimum, and the frequency

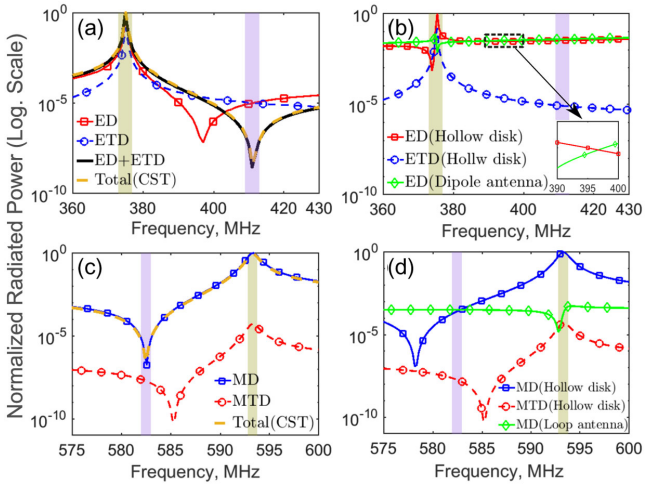

FIG. 3. Cartesian multipole expansion of the radiated power of (a) the NR electric source; (b) the single dipole antenna and the high-index dielectric hollow disk of the NR electric source; (c) the NR magnetic source; (d) the single-loop antenna and the high-index dielectric hollow disk of the NR magnetic source.

411 MHz, where the ED and ETD contributions are equal in magnitude and, due to the last interference term in Eq. (1), provide strong suppression of the total radiated power [see Fig. 3(a)]. To achieve more information, the dipole antenna and hollow disk radiations were separately decomposed to multipoles, and the result is depicted in Fig. 3(b). The separate radiation contributions of the dipole antenna and hollow disk ED moments are equal at the frequency of 397 MHz [see the inset in Fig. 3(b)] and are much higher than the radiated power from ED $(\mathbf{p}_0 + \mathbf{p}_1)$ of the NR electric source [see the red solid line in Fig. 3(a)]. It means that a destructive interference between ED radiations from the dipole antenna and the hollow disk occurs and at this frequency, and we observe the so-called ED-ED anapole state. At the same time, the total electric dipole (ED + ETD) radiation exhibits a strong suppression at 411 MHz, which proves a destructive interference between ED and ETD contributions. Formally, one may conclude that the dip in the radiated power at 411 MHz is obtained due to the ED-ED-ETD anapole state [as shown in Fig. 1(b)], resulting in the existence of the NR electric source at this frequency.

Next, we verify that the same approach can be used to design an NR magnetic source based on the MD-MD anapole state as illustrated in Fig. 1(c). For that purpose, we have incorporated a small magnetic dipole antenna inside an ultrahigh permittivity dielectric hollow disk as shown in Fig. 4(a). Now, the loop antenna radiates as a MD and induces displacement currents inside the hollow disk. We found the conditions when the induced current radiates as another MD moment and its radiation destructively interferes with the MD radiation from the loop antenna. In this case, the radiated power P can be written as [34]

$$P \sim |\mathbf{m}_0 + \mathbf{m}_1|^2 = |\mathbf{m}_0|^2 + |\mathbf{m}_1|^2 + 2\mathrm{Re}[\mathbf{m}_0\mathbf{m}_1^*], \quad (2)$$

where $\mathbf{m}_0$ and $\mathbf{m}_1$ are MD moments of the loop antenna and the hollow disk, respectively, and $(\mathbf{m}_0 + \mathbf{m}_1)$ is the total MD of the system.

The NR magnetic source radiated power over frequency in a comparison to the single-loop antenna in free space is shown in Fig. 4(b). Again, we observe the maximum of the radiated power of the structure at the frequency of 593.5 MHz. It corresponds to the resonance frequency of the dielectric hollow disk (see Sec. II in Supplemental Material [27] for further discussion). The almost zero radiated power occurs at 582.5 MHz. Its magnitude is 3 orders smaller than the radiated power of the single-loop antenna, and, at this condition, we can consider it as an NR magnetic source. The magnetic and electric fields generated by the NR magnetic source and the single-loop antenna at the frequency of 582.5 MHz are shown in Figs. 4(c) and 4(d) and Figs. 4(e) and 4(f), respectively. One may

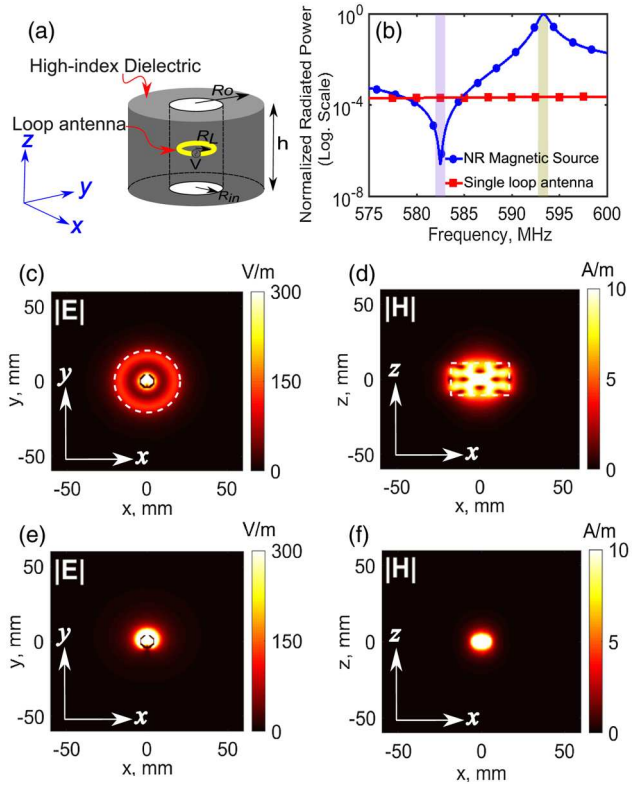

FIG. 4. (a) Schematic view of the NR magnetic source consists of a low-loss ultrahigh permittivity dielectric hollow disk ($\varepsilon = 1000$, $\tan\delta = 2.5 \times 10^{-4}$, $R_0 = 20$ mm, $R_{\text{in}} = 5$ mm, and $h = 20$ mm) and a small copper loop antenna ($R_L = 4$ mm, wire diameter $= 1$ mm). A discrete port with 50 Ω impedance is inserted into the 1 mm slit of the loop antenna. (b) Simulated radiated power of the single-loop antenna in free space and the NR magnetic source over the frequency. (c),(d) Simulated electric and magnetic field distributions of the NR magnetic source. Here, the dashed white lines represent the border of the dielectric hollow disk. (e),(f) Simulated electric and magnetic field distributions of the single-loop antenna in free space.

observe that, in contrast to the isolated loop antenna with field concentration around of the loop position, the NR magnetic source provides the localization of the strong fields inside the disk.

The Cartesian multipole expansion of the NR magnetic source radiated power was also performed. The results are plotted in Figs. 3(c) and 3(d). In accordance with Eq. (2), the total MD contribution is basically defined as the contribution from the MD moment of the single-loop antenna and the MD moment of the dielectric hollow disk. Contributions from other multipoles including the magnetic toroidal dipole (MTD) of the dielectric hollow disk are negligible, as shown in Fig. 3(d). The strong dip in the radiated power at the frequency of 582.5 MHz can be explained by the destructive interference of the contributions from the MD of the single loop and MD of the hollow disk which are crossing each other at this frequency [see Fig. 3(d)], due to the last interference term in Eq. (2), at this spectral point $(|\mathbf{m}_0|^2 + |\mathbf{m}_1|^2) \approx -2\text{Re}[\mathbf{m}_0\mathbf{m}_1^*]$. Thus, one may conclude that we have obtained the MD-MD anapole state which is characterized by low radiation and strong field localization in the near field. The discussion on the matching conditions and near-field enhancement is provided in Sec. II of Supplemental Material [27].

To prove our theoretical predictions, the prototype of the NR electric source was fabricated, and its performance in the near and far-field zone was experimentally investigated (see Fig. 5). To demonstrate applicability of the developed concept even for materials with low refractive index, we have optimized the NR electric source to the microwave frequency range 2–4 GHz. More details are provided in Supplemental Material Sec. V [27]. The fabricated prototype is shown in the inset in Fig. 5(a). The transmittance spectra from the NR electric source to the horn antenna extracted from the measured data as $|S_{21}|^2$ is shown in Fig. 5(b). The pronounced dip of about −80 dB in transmittance at 3.03 GHz corresponds to the predicted ED-ED-ETD anapole state. The measured radiation pattern in the horizontal plane at the maximum and the minimum of the transmittance is compared to the simulated ones in the left and right insets in Fig. 5(b), respectively. The omnidirectional shapes are observed in both cases, but the measured radiation pattern in the right inset does not perfectly match to the simulated results. It can be explained by the low radiated power, which is very hard to detect with the measurement equipment, since it works out of its dynamic range.

The electric field distributions were scanned on the top of the prototype [see Fig. 5(c)]. A good agreement between measured and simulation results is observed. Indeed, at the minimum of transmittance, which corresponds basically to the ED-ED-ETD anapole state, the electric field is strongly localized within the NR electric source.

We have proposed electric and magnetic NR sources based on a single ultrahigh permittivity dielectric hollow disk excited by electric or magnetic pointlike dipole antennas. We have numerically studied the radiation properties of NR sources and revealed that the radiation suppression at the desired frequency is obtained due to the realization of the ED-ED-ETD anapole for the electric NR source and the MD-MD anapole state for the magnetic NR source. We have experimentally confirmed the developed concept on an example of the NR electric source optimized to the microwave frequency range. The proposed NR sources can be viewed as meta-atoms for more complicated nonradiating systems with special functional near-field properties for practical applications in sensing, cloaking, secure communication, RFID tags, wireless power transfer, etc.

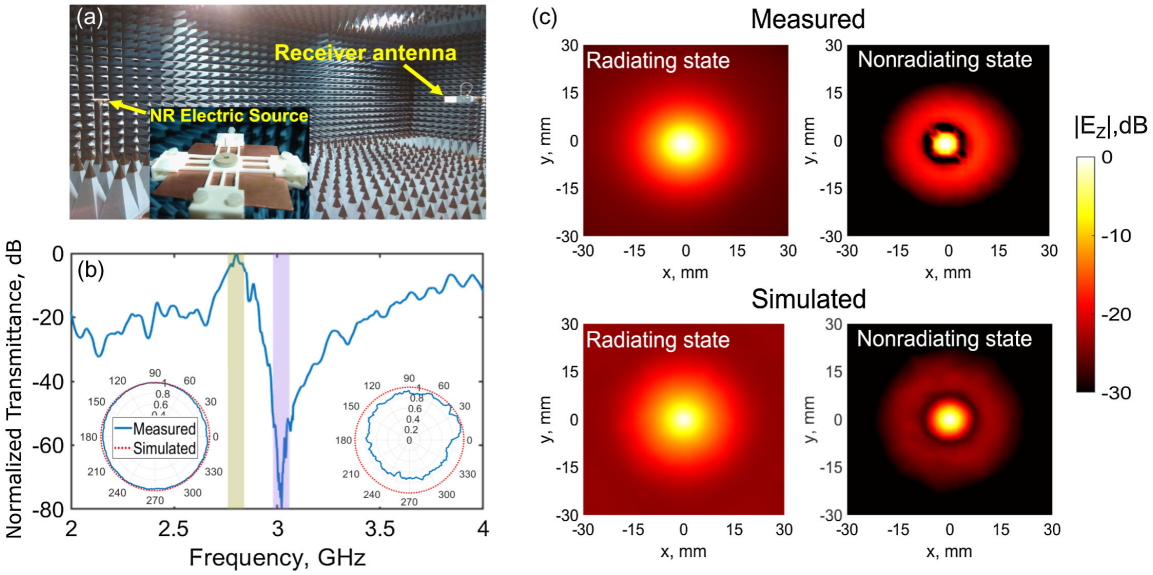

FIG. 5. (a) Experimental setup for the radiation pattern measurements of the NR electric source prototype based on a dielectric hollow disk ($\varepsilon = 235$, $\tan\delta = 2.7 \times 10^{-3}$, $R_{\text{out}} = 6.4$ mm, $R_{\text{in}} = 1.5$ mm, and $h = 4.24$ mm), tightly attached to a copper plate (60×60 mm^2) excited by copper monopole antenna ($L/2 = 18$ mm, wire diameter $= 1$ mm) placed in the center of the hollow disk. (b) The measured spectra of the transmittance. The left and right insets show the measured and simulated radiation patterns of the NR source at the maximum and minimum of the transmittance, respectively. (c) Measured and simulated vertical component of the near electric field distributions 1.5 cm above the NR source prototype. The field amplitudes are normalized to their maximum.

The support from the Deutsche Forschungsgemeinschaft (DFG, German Research Foundation) under Germany's Excellence Strategy within the Cluster of Excellence PhoenixD (EXC 2122, Project ID No. 390833453) is acknowledged. The elaboration of an idea, results of numerical simulation, and experimental investigation of the NR sources were supported by Russian Science Foundation Grant No. 21-79-30038. The multipole analysis of electric and magnetic nonradiating sources was supported by the Russian Science Foundation Grant No. 20-12-00343. E. Z., M. S., and P. K. thank Constantin Simovski and Sergei Tretyakov for discussions.

*a.b.evlyukhin@daad-alumni.de
†andrey.miroshnichenko@unsw.edu.au
‡p.kapitanova@metalab.ifmo.ru

[1] N. Meinzer, W. L. Barnes, and I. R. Hooper, Plasmonic meta-atoms and metasurfaces, Nat. Photonics **8**, 889 (2014).
[2] T. Kaelberer, V. Fedotov, N. Papasimakis, D. Tsai, and N. Zheludev, Toroidal dipolar response in a metamaterial, Science **330**, 1510 (2010).
[3] A. E. Miroshnichenko, A. B. Evlyukhin, Y. F. Yu, R. M. Bakker, A. Chipouline, A. I. Kuznetsov, B. Luk'yanchuk, B. N. Chichkov, and Y. S. Kivshar, Nonradiating anapole modes in dielectric nanoparticles, Nat. Commun. **6**, 8069 (2015).
[4] V. Savinov, N. Papasimakis, D. Tsai, and N. Zheludev, Optical anapoles, Commun. Phys. **2**, 1 (2019).
[5] V. A. Fedotov, A. Rogacheva, V. Savinov, D. P. Tsai, and N. I. Zheludev, Resonant transparency and non-trivial non-radiating excitations in toroidal metamaterials, Sci. Rep. **3**, 2967 (2013).
[6] R. Alaee, C. Rockstuhl, and I. Fernandez-Corbaton, An electromagnetic multipole expansion beyond the long-wavelength approximation, Opt. Commun. **407**, 17 (2018).
[7] E. A. Gurvitz, K. S. Ladutenko, P. A. Dergachev, A. B. Evlyukhin, A. E. Miroshnichenko, and A. S. Shalin, The high-order toroidal moments and anapole states in all-dielectric photonics, Laser Photonics Rev. **13**, 1800266 (2019).
[8] R. Alaee, C. Rockstuhl, and I. Fernandez-Corbaton, Exact multipolar decompositions with applications in nanophotonics, Adv. Opt. Mater. **7**, 1800783 (2019).
[9] J. Chen, J. Ng, Z. Lin, and C. Chan, Optical pulling force, Nat. Photonics **5**, 531 (2011).
[10] I. Fernandez-Corbaton, S. Nanz, R. Alaee, and C. Rockstuhl, Exact dipolar moments of a localized electric current distribution, Opt. Express **23**, 33044 (2015).
[11] Y. Yang and S. I. Bozhevolnyi, Nonradiating anapole states in nanophotonics: From fundamentals to applications, Nanotechnology **30**, 204001 (2019).
[12] A. Devaney and E. Wolf, Radiating and nonradiating classical current distributions and the fields they generate, Phys. Rev. D **8**, 1044 (1973).
[13] P. Pearle, When can a classical electron accelerate without radiating?, Found. Phys. **8**, 879 (1978).
[14] C. W. Hsu, B. Zhen, J. Lee, S.-L. Chua, S. G. Johnson, J. D. Joannopoulos, and M. Soljačić, Observation of trapped light within the radiation continuum, Nature (London) **499**, 188 (2013).

[15] F. Monticone and A. Alu, Embedded Photonic Eigenvalues in 3d Nanostructures, Phys. Rev. Lett. **112**, 213903 (2014).
[16] N. A. Nemkov, A. A. Basharin, and V. A. Fedotov, Nonradiating sources, dynamic anapole, and Aharonov-Bohm effect, Phys. Rev. B **95**, 165134 (2017).
[17] V. A. Zenin, A. B. Evlyukhin, S. M. Novikov, Y. Yang, R. Malureanu, A. V. Lavrinenko, B. N. Chichkov, and S. I. Bozhevolnyi, Direct amplitude-phase near-field observation of higher-order anapole states, Nano Lett. **17**, 7152 (2017).
[18] B. Luk'yanchuk, R. Paniagua-Domínguez, A. I. Kuznetsov, A. E. Miroshnichenko, and Y. S. Kivshar, Hybrid anapole modes of high-index dielectric nanoparticles, Phys. Rev. A **95**, 063820 (2017).
[19] K. Baryshnikova, D. Filonov, C. Simovski, A. Evlyukhin, A. Kadochkin, E. Nenasheva, P. Ginzburg, and A. S. Shalin, Giant magnetoelectric field separation via anapole-type states in high-index dielectric structures, Phys. Rev. B **98**, 165419 (2018).
[20] K. V. Baryshnikova, D. A. Smirnova, B. S. Luk'yanchuk, and Y. S. Kivshar, Optical anapoles: Concepts and applications, Adv. Opt. Mater. **7**, 1801350 (2019).
[21] P. Kapitanova, E. Zanganeh, N. Pavlov, M. Song, P. Belov, A. Evlyukhin, and A. Miroshnichenko, Seeing the unseen: Experimental observation of magnetic anapole state inside a high-index dielectric particle, Ann. Phys. (Berlin) **532**, 2000293 (2020).
[22] A. C. Valero, E. A. Gurvitz, F. A. Benimetskiy, D. A. Pidgayko, A. Samusev, A. B. Evlyukhin, V. Bobrovs, D. Redka, M. I. Tribelsky, M. Rahmani, and K. Z. Kamali, Theory, observation, and ultrafast response of the hybrid anapole regime in light scattering, Laser Photonics Rev.. 2100114 (2021).
[23] A. K. Ospanova, A. Basharin, A. E. Miroshnichenko, and B. Luk'yanchuk, Generalized hybrid anapole modes in all-dielectric ellipsoid particles, Opt. Mater. Express **11**, 23 (2021).
[24] N. A. Nemkov, I. V. Stenishchev, and A. A. Basharin, Nontrivial nonradiating all-dielectric anapole, Sci. Rep. **7**, 1064 (2017).
[25] J. R. Zurita-Sánchez, Anapole arising from a mie scatterer with dipole excitation, Phys. Rev. Research **1**, 033064 (2019).
[26] V. R. Tuz, V. Dmitriev, and A. B. Evlyukhin, Antitoroidic and toroidic orders in all-dielectric metasurfaces for optical near-field manipulation, ACS Appl. Nano Mater. **3**, 11315 (2020).
[27] See Supplemental Material at http://link.aps.org/supplemental/10.1103/PhysRevLett.127.096804 for details of the calculations and measurements, which includes Refs. [28–33].
[28] A. Petosa and A. Ittipiboon, Dielectric resonator antennas: A historical review and the current state of the art, IEEE Antennas Propag. Mag. **52**, 91 (2010).
[29] A. Petosa, *Dielectric Resonator Antenna Handbook* (Artech, London, 2007).
[30] D. M. Pozar, *Microwave Engineering* (John Wiley & Sons, New York, 2011).
[31] E. Nenasheva, N. Kartenko, I. Gaidamaka, O. Trubitsyna, S. Redozubov, A. Dedyk, and A. Kanareykin, Low loss microwave ferroelectric ceramics for high power tunable devices, J. Eur. Ceram. Soc. **30**, 395 (2010).
[32] E. Nenasheva, N. Kartenko, I. Gaidamaka, S. Redozubov, A. Kozyrev, and A. Kanareykin, Low permittivity ferroelectric composite ceramics for tunable applications, Ferroelectrics **506**, 174 (2017).
[33] N. Shipman, J. Bastard, M. Coly, F. Gerigk, A. Macpherson, N. Stapley, G. Burt, and A. Castilla, A ferroelectric fast reactive tuner for superconducting cavities, in *Proceedings of the Superconducting RF Workshop, SRF* (JACoW Publishing, Geneva, 2019), pp. 5–9.
[34] A. B. Evlyukhin, T. Fischer, C. Reinhardt, and B. N. Chichkov, Optical theorem and multipole scattering of light by arbitrarily shaped nanoparticles, Phys. Rev. B **94**, 205434 (2016).
[35] P. D. Terekhov, K. V. Baryshnikova, Y. A. Artemyev, A. Karabchevsky, A. S. Shalin, and A. B. Evlyukhin, Multipolar response of nonspherical silicon nanoparticles in the visible and near-infrared spectral ranges, Phys. Rev. B **96**, 035443 (2017).